First-Principle Calculation of the Recombination Cross-Section Assisted by Acoustic Phonons at Shallow Impurities in Semiconductors.

L. REGGIANI and L. VARANI

Dipartimento di Fisica e Centro Interuniversitario di Struttura della Materia dell'Università di Modena - Via Campi 213/A, 41100 Modena, Italia

V. MITIN

Institute of Semiconductors, Academy of Sciences of the Ukrainian SSR - Kiev, USSR

(ricevuto il 23 Luglio 1990)

Summary. — An original Monte Carlo study of the equilibrium microscopic and macroscopic recombination cross-sections at shallow impurity centres is presented. Both cross-sections are investigated in lightly doped p-Si as functions of the temperature and ionized acceptor concentration. In order to treat generation-recombination processes we extend the semi-classical Boltzmann equation through a simulation of the carrier motion in the energy-configuration space of an impurity centre. The analysis of the scattering rates as a function of the total carrier energy enables a microscopic interpretation of the capture process to be carried out. The role of excited levels is naturally included and found to be of main importance at increasing lattice temperatures. Numerical results are then compared with available experiments and existing analytical calculations.

PACS 72.10.i – Theory of electronic transport: scattering mechanisms.
PACS 72.20.Jv – Charge carriers: generation, recombination, lifetime, and trapping.
PACS 72.80.Cw – Elemental semiconductors.

1. – Introduction.

The recombination cross-section at shallow impurity centres assisted by acoustic phonons is one of the most important physical quantities in determining the extrinsic transport properties in semiconductors at low temperatures. The cascade-capture model, originally introduced by Lax [1] and further elaborated by the Leningrad group [2-4], is at the basis of the theoretical investigation of existing experimental results. (Attempts to improve the cascade model allowing for the quantum nature of transitions between energy levels have also been reported in ref. [5]. However, the calculated cross-section was in large disagreement with experiments.) Despite

significant success in interpreting experiments, the analytical approaches used so far are, however, subjected to the following limitations. Within Lax's approach [1] one has to resort to the sticking function. This function accounts at a kinetic level for the probability a carrier has to finally reach the ground state of the impurity without returning to the conducting band, and its determination remains a complicated affair [6-10]. As a result, the effect of excited impurity levels during recombination remains hidden in spite of its recognized importance in determining the dynamics of recombination [11] and low-temperature breakdown phenomena [12]. The Leningrad group [2-4] has made use of a phenomenological energy-relaxation time to solve the appropriate kinetic equation. They succeeded in providing analytical results of the average capture cross-section, but only in the two asymptotic regions $KT \ll ms^2$ and $KT \gg ms^2$ (m and s being the effective mass and the sound velocity, respectively). As a consequence, in the intermediate region $KT \simeq ms^2$, which for the case of p-Si treated here corresponds to the interesting temperature region centred around 2 K, a simple interpolation formula for the average capture cross-section has been provided. Furthermore, the energy dependence of the differential capture cross-section is still subject to controversy [13].

The aim of this paper is to present a new approach which, being free from the above limitations, offers a more direct physical interpretation and opens new possibilities of investigation. It consists in a simulation of the carrier motion in the energy-configuration space of an impurity centre, thus resembling a molecular dynamics calculation.

The paper is organized as follows: sect. 2 presents the theoretical model for the evaluation of the scattering rates as a function of the carrier total energy. In sect. 3 the main features of the Monte Carlo simulation of the carrier motion in the energy-configuration space of an impurity centre are presented. The problem of the determination of the recombination cross-section is discussed in sect. 4. Section 5 reports our results for the average and differential cross-sections and a comparison with the experiments and the analytical calculations available in the literature. The main conclusions are drawn in sect. 6.

2. – Theoretical model.

The calculation of the recombination cross-section is based on a simulation of the carrier motion in a total energy space, as shown schematically in fig. 1, where we assume that the positive energy region corresponds to conducting states while the negative energy region to bound states. This scheme accounts for both the kinetic energy of the carrier and the potential energy of the impurity $U(r)$ given by

$$U(r) = -\frac{e^2}{4\pi K K_0 r}, \tag{1}$$

where e is the electron charge with its sign, K the relative static dielectric constant of the material and K_0 the vacuum permittivity.

Accordingly, the carrier kinetic energy ε can be written as

$$\varepsilon = E_0 - U(r) = E_0 + E_0^f/x - E_0^f, \tag{2}$$

where E_0 is the carrier total energy (or simply the energy), $E_0^f = e^2/4\pi K_0 K r_I$ is the

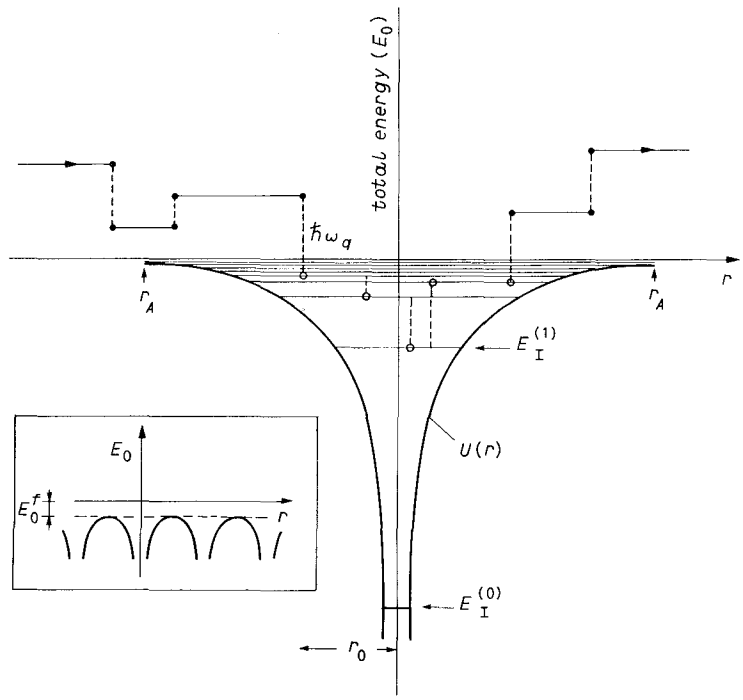

Fig. 1. – Schematic representation of a trajectory of an electron in the (total) energy space at equilibrium. The full dots mark scattering processes via phonons with energy $\hbar\omega_q$ that an electron undergoes in the positive energy region where it moves freely. In the attractive Coulomb field $U(r)$ it is accelerated and at the distance r_0 (measured from the charged centre) the electron enters the negative energy region. The open dots mark transitions between the energy levels of the impurity centre in the negative energy region where the electron is considered as trapped. All transitions are assumed to occur instantaneously in space and time (transitions in the negative energy region are supposed to occur at the impurity site). The insert shows the energy level E_0^f associated with the fluctuational Coulomb potential of the impurity.

Coulomb energy at $r = r_I$ (with $r_I = (N_I^-)^{-1/3}$ the mean radius of one impurity) due to the randomly distributed impurities, N_I^- is the ionized impurity concentration, $x = r/r_I$ is a dimensionless distance. In eq. (2) the energy is measured from $-E_0^f$ to account for the fact that the carrier is really bound only for $E_0 < -E_0^f$ because of the overlap among different impurity centres.

As long as the distance between the excited levels around KT (K being the Boltzmann constant and T the lattice temperature) is negligible with respect to both the ionization energy $E_I^{(0)}$ and the thermal energy KT, the energy region from the bottom of the conducting band to, let us say, the first ionized level $E_I^{(1)} = E_I^{(0)}/4$ can be considered as a continuum spectrum. Therefore, within the temperature range $KT < E_I^{(1)}$, the semi-classical approach (Boltzmann equation) can be applied in the whole energy region covering the conducting and the bound states [3].

To perform the simulation in the total energy space, we evaluate the scattering rate as a function of the carrier total energy. This is accomplished by making a space average which, for a single Coulomb centre, is given by the following rule [3]: given a

TABLE I. – *Parameters for p-Si used in calculations* [15], m_0 *is the free electron mass.*

effective mass	$m_h = 0.53 \div 1.26\, m_0$
crystal density	$\varrho_0 = 2.32\,\mathrm{g\,cm^{-3}}$
sound velocity	$s = 6.53 \cdot 10^5\,\mathrm{cm\,s^{-1}}$
relative static dieletric constant	$\kappa = 11.7$
acoustic deformation potential	$E_1^0 = 5\,\mathrm{eV}$
energy of the impurity ground state	$E_I^{(0)} = 45\,\mathrm{meV}$

function $A(\varepsilon)$, the corresponding $A(E_0)$ is determined as

$$A(E_0) = \langle A(\varepsilon)\rangle_{\mathrm{space}} = \frac{\int_0^{r_{\max}} A(\varepsilon)\, r^2\, \mathrm{d}r}{\int_0^{r_A} r^2\, \mathrm{d}r} = 3 \int_0^{x_{\max}} A(E_0 + E_0^f/x - E_0^f)\, x^2\, \mathrm{d}x\,, \tag{3}$$

where the integration domain is the volume belonging to one impurity and $x_{\max}$ is

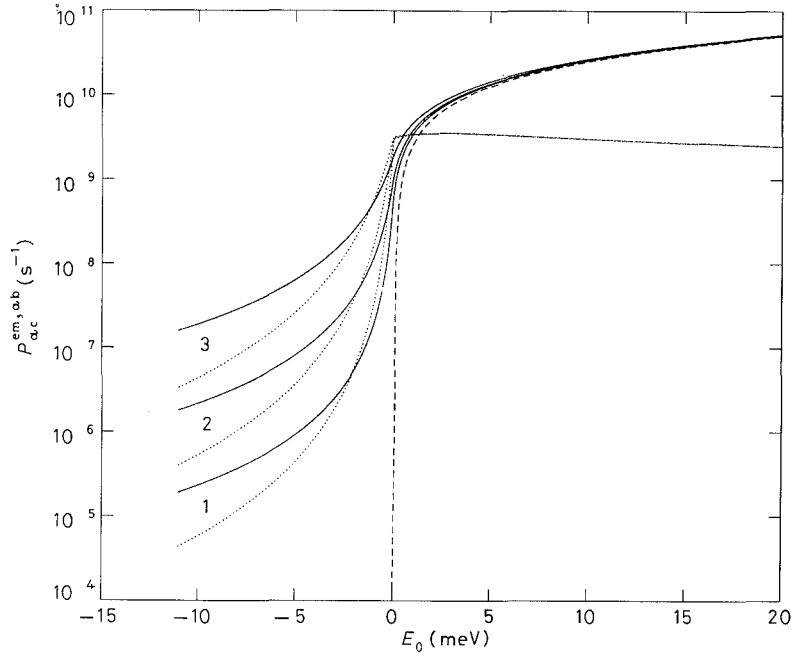

Fig. 2. – Scattering rates as functions of the (total) carrier energy in p-type Si for a temperature $T = 10\,\mathrm{K}$. The continuous and dotted curves refer to the processes of acoustic-phonon emission and absorption, respectively. The couples of curves labelled 1, 2 and 3 are obtained for an ionized acceptor concentration of respectively $N_A^- = 10^{13}$, 10^{14} and $10^{15}\,\mathrm{cm^{-3}}$. The dashed line refers to the scattering rate for the process of acoustic-phonon emission for $N_A^- = 0$. The curve for the process of acoustic-phonon absorption for $N_A^- = 0$ is found to nearly coincide with the dotted curves for $E_0 \geqslant 0$.

determined by the constraint $\varepsilon \geqslant 0$, *i.e.*

$$x_{\max} = 1 \quad \text{for } E_0 \geqslant -E_0^f \quad \text{and} \quad x_{\max} = -\frac{E_0^f}{E_0 - E_0^f} \quad \text{for } -E_1^{(1)} \leqslant E_0 < -E_0^f \text{ (*)}.$$

The above scheme is applied to the case of p-type silicon at temperatures below 77 K so that the condition $KT < E_1^{(1)}$ is fulfilled. A single spherical band model, the heavy holes, with a temperature-dependent effective mass m_h which accounts for nonparabolic effects, is used [14]. We remark that, being at equilibrium, we do not need to follow the momentum of carriers so that only changes of E_0 due to scatterings are important. Therefore, elastic-scattering mechanisms, such as ionized impurities, can be neglected in the simulation. Table I reports the values of the parameters used in the simulation [15].

Figure 2 shows the energy dependence of the scattering rates for acoustic-phonon emission and absorption processes at the temperature of $T = 10$ K for the ionized

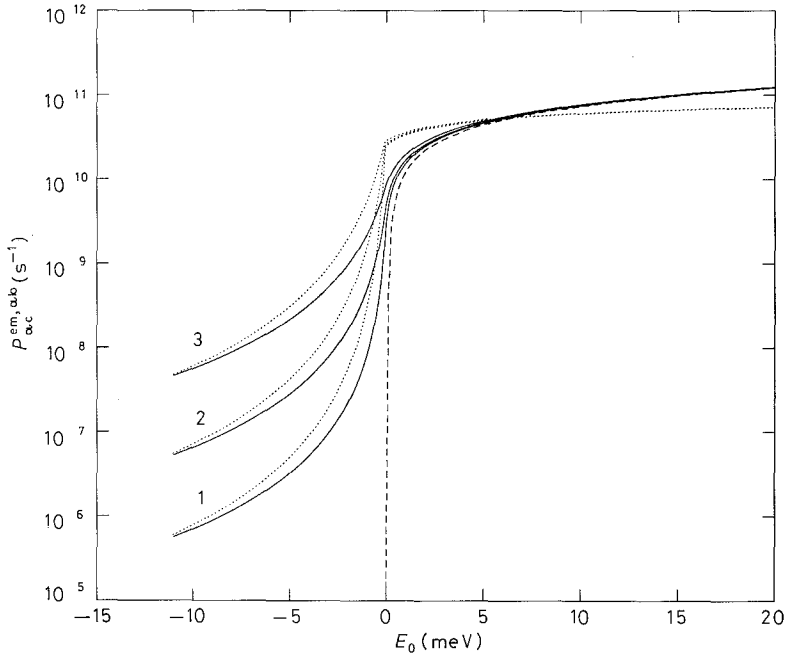

Fig. 3. – Scattering rates as a function of the (total) carrier energy in p-type Si for a temperature $T = 50$ K. The continuous and dotted curves refer to the processes of acoustic-phonon emisssion and absorption, respectively. The couples of curves labelled 1, 2 and 3 are obtained for an ionized acceptor concentration of, respectively, $N_A^- = 10^{13}$, 10^{14} and 10^{15} cm^{-3}. The dashed line refers to the scattering rate for the process of acoustic-phonon emission for $N_A^- = 0$. The curve for the process of acoustic-phonon absorption for $N_A^- = 0$ is found to nearly coincide with the dotted curves for $E_0 \geqslant 0$.

(*) Here the Coulomb potential for a single impurity has been cut off at $-E_0^f$. However, more generally, the Coulomb potential for a single impurity should be cut off at the percolation energy value [10], which leads to a somewhat larger volume average than in our case.

acceptor concentrations respectively of $N_A^- = 10^{13}$, 10^{14} and 10^{15} cm^{-3}. Figure 3 shows analogous results at $T = 50$ K.

As seen from these figures, the presence of the impurities is responsible for a tail of the scattering rates in the negative energy region, this tail being more pronounced at increasing concentrations. We notice that at $T = 10$ K (see fig. 2) the curves corresponding to P_{ac}^{em} and P_{ac}^{ab} cross in two points which slightly depend on the ionized acceptor concentration: one in the positive and the other in the negative energy region; we denote the corresponding energies E_0^+ and E_0^-, respectively. In the positive energy region, when $E_0 \geqslant E_0^+$ it is $P_{ac}^{em} \geqslant P_{ac}^{ab}$ and, when $E_0 < E_0^+$, it is $P_{ac}^{em} < P_{ac}^{ab}$. This behaviour of the scattering rates implies that, while wandering in the positive-energy region the carrier mean energy, as expected by detailed balance, always relaxes to $3KT/2$ which is close to E_0^+.

In the negative energy region when $E_0 \leqslant E_0^-$ it is $P_{ac}^{em} \geqslant P_{ac}^{ab}$ and, when $E_0 > E_0^-$, it is $P_{ac}^{em} < P_{ac}^{ab}$. This behaviour of the scattering rates implies that while wandering in the negative energy region if $E_0 > E_0^-$ absorption processes prevail and the carrier tends to come back in the conducting band thus being generated (pseudogenerated because to have a true generation the carrier should come from the ground state). On the contrary, if $E_0 \leqslant E_0^-$ emission processes prevail and the carrier tends to penetrate more deeply in the negative energy region, thus finally sticking to the ground state of the impurity levels (true recombination).

The situation is different at $T = 50$ K (see fig. 3): here the scattering rates have only the crossing point (E_0^+) in the positive-energy region. Therefore, at high temperature carriers exhibit the tendency to go to the conducting band rather than to the ground state of the impurity from any excited state.

3. – Monte Carlo simulation.

The Monte Carlo procedure follows the standard steps [16]. A carrier with initial thermal energy makes stochastic free flights determined with the self-scattering procedure. Absorption and emission processes are determined according to their respective rates. Once a process is selected, the energy of the acoustic phonon involved in the transition should be determined. To this end, we must evaluate the kinetic energy of the carrier just before scattering. This is a complicate problem, because from eq. (2) the kinetic energy strongly depends on the position of the carrier with respect to the impurity centre. For this purpose, we have devised the following procedure. Just before the scattering we evaluate the minimum value attainable by the kinetic energy $\varepsilon_{min} = E_0 + E_0^f/x_{max} - E_0^f$. The position of the carrier relative to the impurity centre, x_r, is then selected as uniformly distributed between x_{min} and x_{max} with the rule

$$x_r = x_{min} + (x_{max} - x_{min})\, r\,, \tag{4}$$

where $x_{min} = E_0^f/E_{max}$ (E_{max} is the maximum value of the energy considered in the simulation) and r is a random number uniformly distributed between 0 an 1.

For absorption processes, the corresponding value of $\varepsilon(x_r) = \varepsilon_r$ is accepted provided the following rejection condition, which weigths appropriately the absorption probability with the available phase space, is satisfied:

$$P_{ac}^{ab}(\varepsilon_r)\, x_r^2 / [P_{ac}^{ab}(\varepsilon_{min})\, x_{max}^2] > r\,. \tag{5}$$

For emission processes, the value of ε_r is analogously accepted provided the following rejection condition is satisfied:

$$P_{ac}^{em}(\varepsilon_r)\, x_r^2 / f_{ac}^{em}(\varepsilon_r) > r \tag{6}$$

with

$$\begin{cases} f_{ac}^{em}(\varepsilon_r) = P_{ac}^{em}(\varepsilon_{min})\, x_{max}^2 , & \text{for } \varepsilon_r \geq 3 m_h s^2 , \\ f_{ac}^{em}(\varepsilon_r) = f_{max} , & \text{for } \varepsilon_r < 3 m_h s^2 . \end{cases} \tag{7}$$

Since for emission processes $P_{ac}^{em}(\varepsilon_r) \to 0$ for $\varepsilon_r \to 0$, the maximum value of $P_{ac}^{em}(\varepsilon_r)\, x^2$, here called f_{max}, is determined numerically in the lowest-energy region $\varepsilon_r < 3 m_h s^2$.

The energy of the acoustic phonon involved in the transition is then determined with the following procedure. Let us consider the case of the absorption processes. From the knowledge of the carrier kinetic energy just before scattering, ε_r, the phonon energy ε_q, which in the dimensionless variable y is given by $\varepsilon_q = y\, KT$, is generated as uniformly distributed within the range of values allowed by momentum and energy conservation, $y_m^{ab} \leq y \leq y_M^{ab}$, as

$$y = (y_M^{ab} - y_m^{ab})\, r + y_m^{ab} \tag{8}$$

with

$$\begin{cases} y_m^{ab} = 0 , & \text{for } y_r \geq y_s , \\ y_m^{ab} = 4(y_s - y_r)\, y_s , & \text{for } y_r < y_s , \end{cases} \tag{9}$$

$$y_M^{ab} = 4(y_r + y_s)\, y_s , \tag{10}$$

where $y_r = (\varepsilon_r / KT)^{1/2}$ and $y_s = (m_h s^2 / 2KT)^{1/2}$.

The value of y so determined is accepted provided the following rejection condition, which accounts for the appropriate joint probability of finding the phonon energy for a given carrier energy, is satisfied:

$$\frac{y^2}{\exp[y] - 1} < g(y_M^{ab})\, r , \tag{11}$$

where

$$\begin{cases} g(y_M^{ab}) = (y_M^{ab})^2 / [\exp[y_M^{ab}] - 1] , & \text{for } y_M^{ab} \leq 1.6 , \\ g(y_M^{ab}) = 0.65 , & \text{for } y_M^{ab} > 1.6 , \end{cases} \tag{12}$$

For emission processes, the energy of the acoustic phonon involved in the transition is obtained in an analogous way. In this case, y is generated as uniformly distributed within the allowed range of values $0 \leq y \leq y_M^{em}$ as

$$y = y_M^{em}\, r \tag{13}$$

with

$$y_M^{em} = 4(y_r - y_s)\, y_s . \tag{14}$$

The value so determined is accepted provided the following rejection condition is satisfied:

$$\frac{y^2}{1-\exp[-y]} < \frac{(y_M^{em})^2}{1-\exp[-y_M^{em}]} r . \tag{15}$$

4. – Determination of the recombination cross-section.

The determination of the (velocity) average capture cross-section $\bar{\sigma}_{ac}$ follows from its definition in terms of the recombination time, τ_r, through the standard relationship [3, 17]

$$\bar{\sigma}_{ac} = \tau_r N_A^- \langle v \rangle^{-1} , \tag{16}$$

where $\langle v \rangle = \sqrt{8KT/\pi m_h}$ is the average velocity of carriers at equilibrium.

Thus the main task of the present approach is to define τ_r. The most natural way of doing so is to calculate τ_r from the ratio between the time the carrier spends in the valence band and the number of transitions which the carrier undergoes in the negative-energy region. For illustrative purposes, fig. 4 reports an excerpt of the time evolution of the carrier energy as given by the Monte Carlo simulation for a temperature $T = 10\,\mathrm{K}$ and an ionized acceptor concentration $N_A^- = 10^{13}\,\mathrm{cm}^{-3}$. In the negative-energy region the carrier has two possibilities: i) to spend some time in the upper excited levels and then come back to the conducting band; ii) to penetrate far in

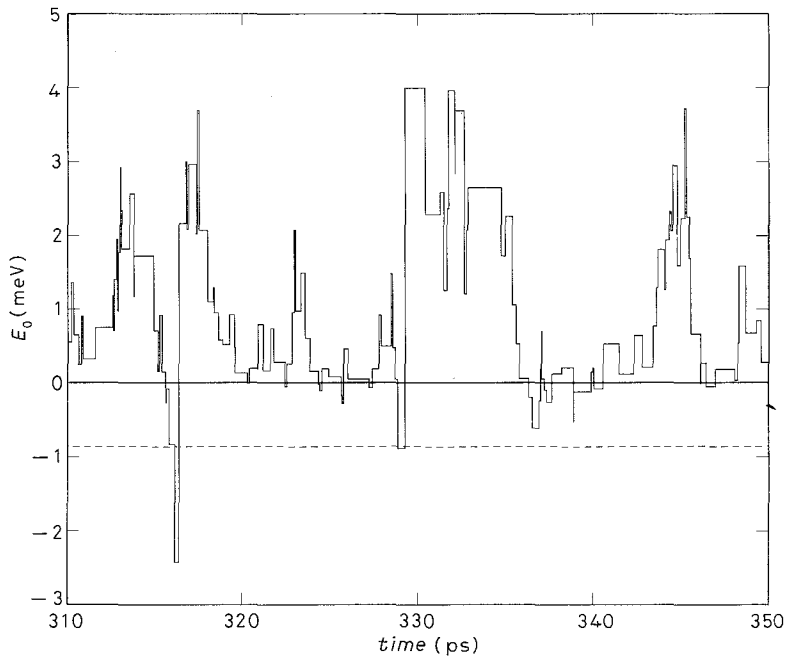

Fig. 4. – Excerpt of the time evolution of the carrier (total) energy as given by the Monte Carlo simulation for a temperature $T = 10\,\mathrm{K}$ and an ionized acceptor concentration $N_A^- = 10^{13}\,\mathrm{cm}^{-3}$. The dashed line represents the energy level $E_0 = -KT$ for $T = 10\,\mathrm{K}$.

the negative-energy region, that is where $E_0 \leqslant -KT$. Both these possibilities are shown in fig. 4.

Case ii) corresponds to the concept of a real capture and, when this occurs, we stop the simulation of the given particle and generate a new one in the conducting band with a velocity determined from detailed balance. Detailed balance is accounted for with the following self-consistent procedure. When, because of acoustic absorption process, the carrier will go from the negative- to the positive-energy region, we have a generation (pseudogeneration). Accordingly, we construct the normalized histogram of the number of transitions to the positive-energy region per unit energy interval $\mu(E_0)$. These histograms, which are shown in fig. 5 and 6 for the different temperatures and impurity concentrations reported, are then consistently used to determine stochastically the final energy of the new carrier generated in the conducting band according to case ii). All the histograms exhibit a maximum just below 0.5 meV while for increasing energies they tend to zero. The energy at which the curves reach their maximum values is associated with the average phonon energy involved in the transition which is of the order of $\sqrt{KTm_h s^2}$. Indeed this energy slightly shifts at higher values with increasing temperature for a given impurity concentration (see fig. 5). The tails of the three curves for increasing carrier energies are more pronounced at both increasing temperatures and impurity concentrations. In this latter case (see fig. 6) this effect is associated to the increased density of states in and near to the zero (total) energy region.

In accordance with the above two possibilities we introduce two different times of

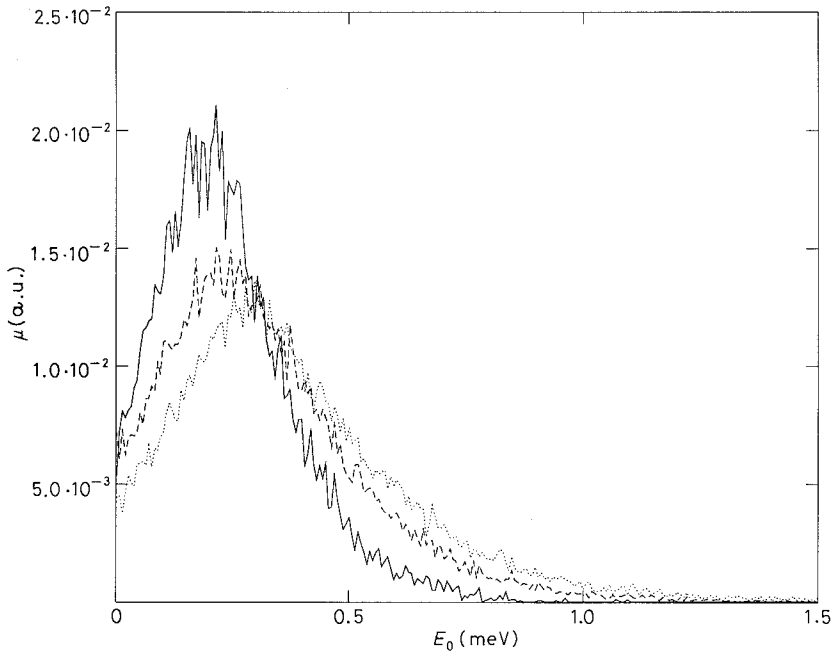

Fig. 5. – Normalized histogram of the number of transitions from the negative to the positive (total) energy region as a function of the (total) carrier energy as obtained from the Monte Carlo simulation in p-type Si for an ionized acceptor concentration $N_A^- = 10^{13}$ cm^{-3}. The continuous, dashed and dotted curves refer to the temperatures of, respectively, $T = 2$, 10 and 50 K.

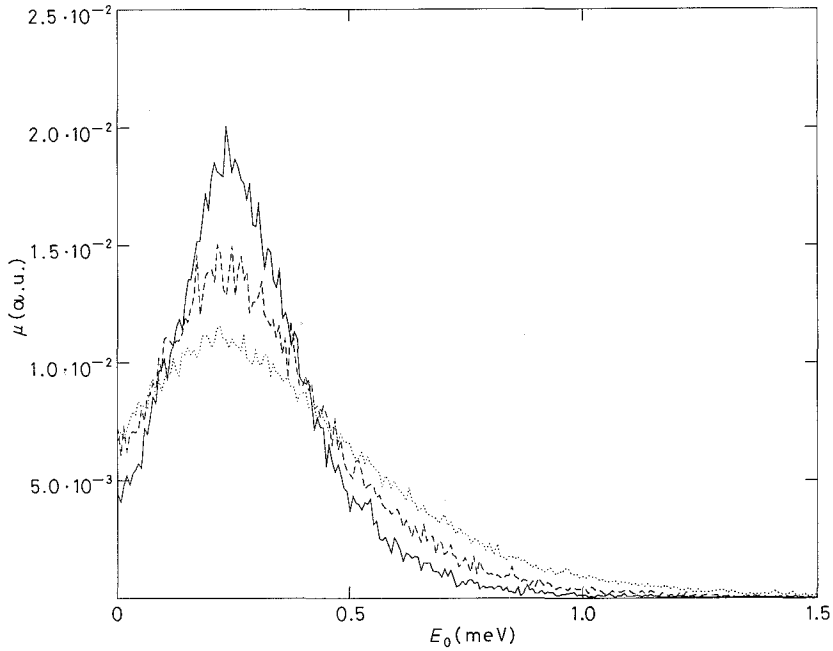

Fig. 6. – Normalized histogram of the number of transitions from the negative to the positive (total) energy region as a function of the (total) carrier energy as obtained from the Monte Carlo simulation in p-type Si for a temperature $T = 10\,\mathrm{K}$. The continuous, dashed and dotted curves refer to the ionized acceptor concentrations of, respectively, $N_A^- = 10^{12}$, 10^{13} and $10^{14}\,\mathrm{cm}^{-3}$.

recombination, τ_{r1} and τ_{r2}, which, from eq. (4), define two different cross-sections $\bar{\sigma}_{1ac}$ and $\bar{\sigma}_{2ac}$. While the former accounts for all the transitions to $E_0 \leqslant 0$, the latter accounts only for those transitions, among the former ones, which lead the carrier along the ladder of excited levels to $E_0 \leqslant -E_c$, where E_c is a cut-off energy of the order of KT. As a general trend it is $\bar{\sigma}_{2ac} \leqslant \bar{\sigma}_{1ac}$ and $\bar{\sigma}_{2ac}$ depends on the value of E_c; in any case, as we shall see later, the value of $\bar{\sigma}_{2ac}$ tends to saturate at increasing values of E_c.

Finally, by constructing the normalized histogram of the number of transitions to the negative energy region for a given initial energy, $\nu_1(E_0)$, the simulation enables us to determine the differential capture cross-section $\sigma_{ac}(E_0)$ as a function of the carrier energy which, for the case i), is given by

$$\sigma_{1ac}(E_0) = \frac{KT}{E_0} \exp\left[\frac{E_0}{KT}\right] \frac{2}{\sqrt{\pi}} \bar{\sigma}_{1ac}\, \nu_1(E_0)\,. \tag{17}$$

It is easily verified that eq. (17) satisfies the definition of $\bar{\sigma}_{1ac}$ given by

$$\bar{\sigma}_{1ac} = \langle \sigma_{1ac}(E_0)\, v(E_0) \rangle / \langle v(E_0) \rangle\,. \tag{18}$$

Of course, an analogous procedure can be used to determine $\sigma_{2ac}(E_0)$. Figures 7 and 8 show $\nu_1(E_0)$ for the temperatures and the ionized acceptor concentrations reported, respectively. Again all the histograms exhibit a maximum while for increasing energies they tend to zero. The physical reasons for this behaviour are the same as for

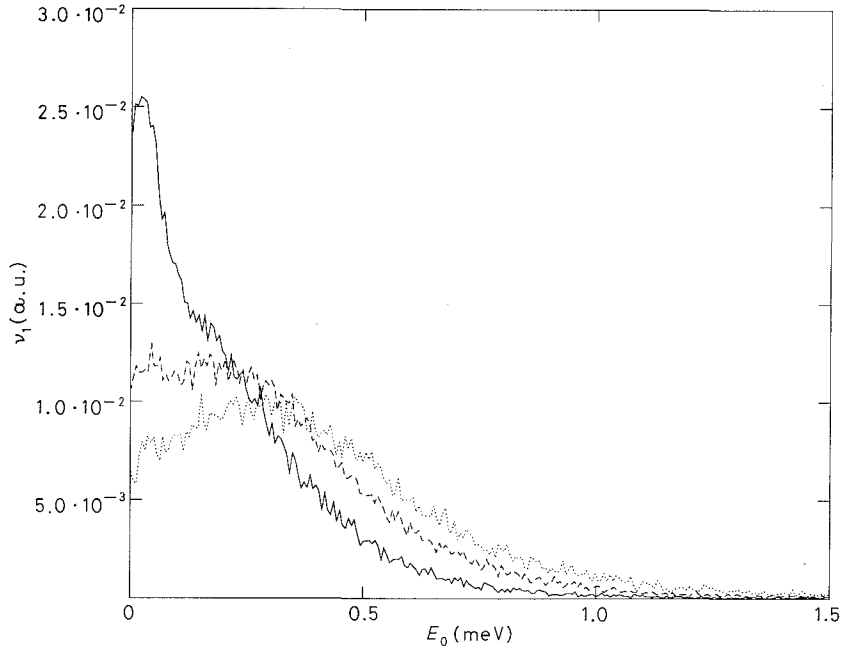

Fig. 7. – Normalized histogram of the number of transitions from the positive to the negative (total) energy region as a function of the (total) carrier energy as obtained from the Monte Carlo simulation in p-type Si for an ionized acceptor concentration $N_A^- = 10^{13}$ cm^{-3}. The continuous, dashed and dotted curves refer to the temperatures of, respectively, $T = 2$, 10 and 50 K.

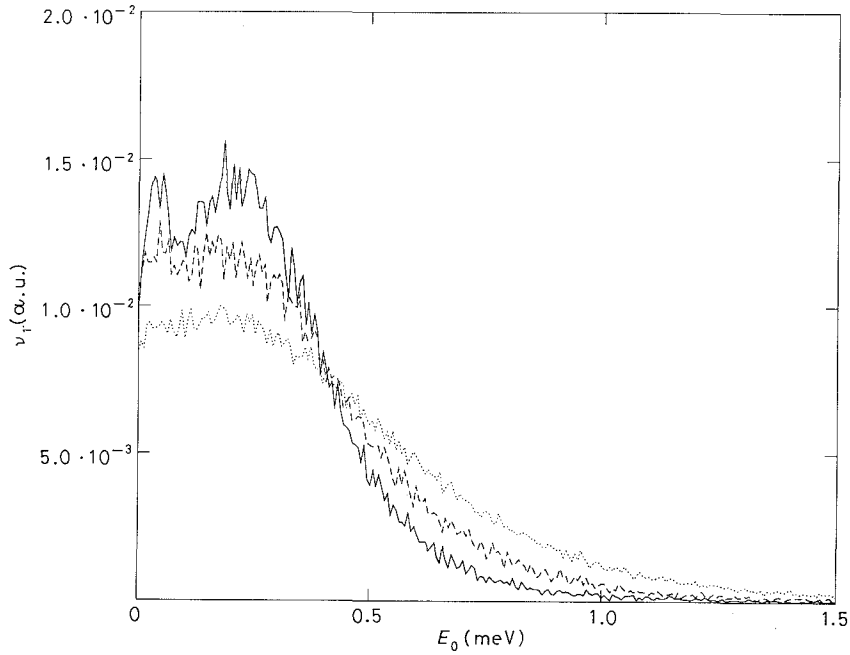

Fig. 8. – Normalized histogram of the number of transitions from the positive to the negative (total) energy region as a function of the carrier (total) energy as obtained from the Monte Carlo simulation in p-type Si for a temperature $T = 10$ K. The continuous, dashed and dotted curves refer to the ionized acceptor concentrations of respectively $N_A^- = 10^{12}$, 10^{13} and 10^{14} cm^{-3}.

the histograms of $\mu(E_0)$ (see fig. 5, 6). According to eqs. (3.1)-(3.3) of ref. [17] it is easy to show that $\nu_1(E_0)$ represents the normalized probability of recombination at equilibrium for a carrier with energy E_0.

5. – Results and discussion.

A significant test of the procedure used is the calculation of the energy distribution functions. We have found a good agreement with the expected Maxwell-Boltzmann shape, apart from the lowest negative energy region. Here, because of the cut-off procedure and the numerical uncertainty in the determination of the density of states, the expected shape cannot be reproduced. Overall the general agreement found supports the physical plausibility of the procedure here used.

Figure 9 shows the dependence of $\bar{\sigma}_{2ac}$ on E_c as obtained from calculations. It demonstrates that in most cases the high excited states exchange carriers in practice only with the conducting band. We believe that the saturation value of $\bar{\sigma}_{2ac}$ should be taken as the recombination average cross-section associated with the true capture.

The temperature dependence of the two average capture cross-sections defined above is shown in fig. 10, together with the analytical result of eq. (5) in ref. [3] and with available results in the literature referring to the shallow acceptors boron and gallium. Theoretical calculations, which have been performed for an ionized acceptor concentration $N_A^- = 10^{13}\ \mathrm{cm}^{-3}$, show that $\bar{\sigma}_{2ac}$ is systematically smaller than $\bar{\sigma}_{1ac}$. Furthermore, the dependence on temperature of the former exhibits a steeper decreasing behaviour. Consistent with our model, these results reflect the different role we have attributed to the excited states in defining the average capture

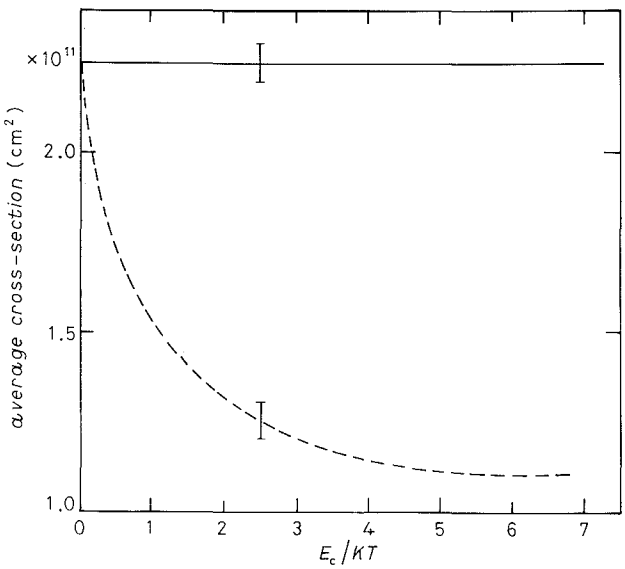

Fig. 9. – Average capture cross-sections in p-type Si as a function of the cut-off energy in the negative-energy region for an ionized acceptor concentration $N_A^- = 10^{13}\ \mathrm{cm}^{-3}$ and a temperature $T = 2\,\mathrm{K}$. Continuous and dashed lines represent $\bar{\sigma}_{1ac}$ and $\bar{\sigma}_{2ac}$, respectively (see the text). Bars indicate the uncertainty of the calculations.

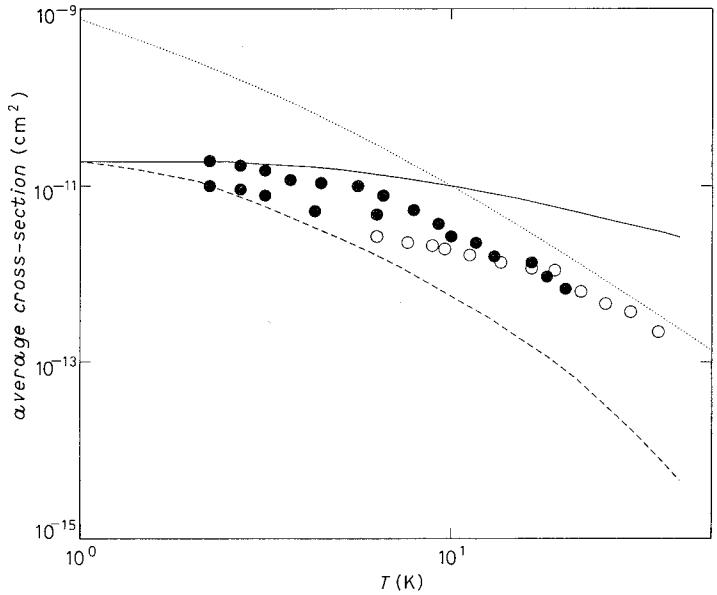

Fig. 10. – Average capture cross-section in p-type Si at equilibrium as a function of temperature. Curves report the present calculations performed for $N_A^- = 10^{13}\,\mathrm{cm}^{-3}$ and symbols the experiments of various authors [3]. The continuous and dashed lines refer to $\bar{\sigma}_{1ac}$ and $\bar{\sigma}_{2ac}$ obtained for $E_c = -KT$, respectively (see the text). The dotted line represents the behaviour predicted by eq. (5) of ref. [3] obtained with an effective mass $m_h = 0.53\,m_0$.

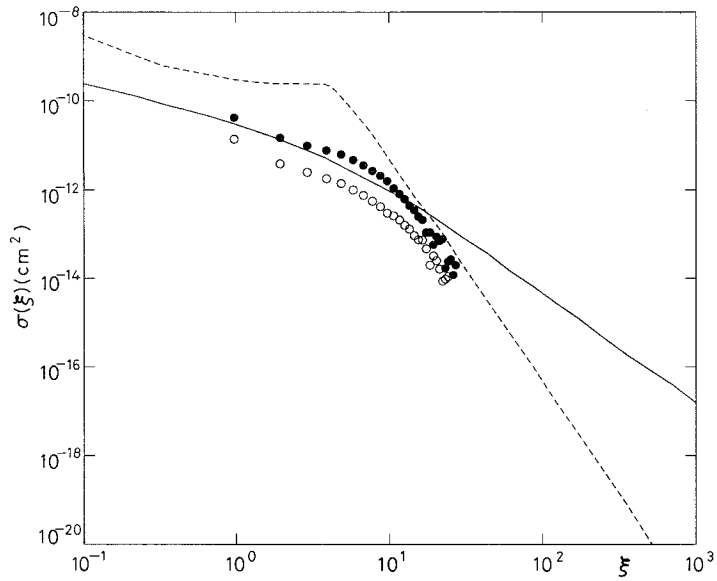

Fig. 11. – Differential capture cross-section in p-type Si as a function of the dimensionless energy $\xi = 2E_0/m_h s^2$ at $T = 5\,\mathrm{K}$. Symbols report the results of the Monte Carlo simulation obtained for an ionized acceptor concentration $N_A^- = 10^{13}\,\mathrm{cm}^{-3}$; full and open circles refer to $\bar{\sigma}_{1ac}$ and $\bar{\sigma}_{2ac}$, respectively (see the text). Continuous and dashed curves report the analytical calculations of Lax and Khan-Bhattacharya models, respectively [14].

cross-sections. We notice that the experimental results lie between the two theoretical curves and that, at lowering temperatures, Monte Carlo results agree with experiments better than formula of ref. [3]. However, the fundamental question arises: what do experiments really measure? It can easily be argued that, as a general trend, the experiments should measure something intermediate between $\bar{\sigma}_{1ac}$ and $\bar{\sigma}_{2ac}$, this latter quantity representing a smallest asymptotic limit. Indeed, a more critical use of eq. (16), for what concerns the physical meaning of the characteristic time the experimentalists substitute for τ_r, should lead to a reinterpretation of most of the data appeared in the literature. Thus, we conclude that our calculations provide a physically well-founded scheme for the interpretation of the recombination cross-section at shallow impurity levels. In particular, we do not need to exploit the sticking function (which has been an open source of controversy in the leterature [1-10]), since sticking processes are self-consistently accounted for in our simulation.

The energy dependence of the recombination cross-sections calculated from eq. (17) are reported in fig. 11 together with the analytical results of Lax [1] and Khan-Bhattacharya [13]. Here, for the purpose of providing a universal formulation, the dimensionless energy $\xi = 2E_0/m_h s^2$ is introduced. According to the results for the average cross-sections, $\sigma_{1ac}(\xi)$ is systematically larger than $\sigma_{2ac}(\xi)$. Furthermore, both $\sigma_{1ac}(\xi)$ and $\sigma_{2ac}(\xi)$ exhibit a steeply decreasing dependence with increasing energy, which reflects the dominant importance of low energetic carriers in the process of recombination. We notice that present results are intermediate between those of ref. [1] and [13]. Indeed, at low energies we agree with [1] while at higher energies the present results better follow those of [13].

The present calculations enable us to investigate also the dependence of the average capture cross-section on the impurity concentration. Our results for $10^{10}\,\mathrm{cm}^{-3} \leqslant N_A^- \leqslant 10^{15}\,\mathrm{cm}^{-3}$, which are reported in fig. 12, show that $\bar{\sigma}_{1ac}$ increase almost linearly at decreasing ionized impurity concentrations, while $\bar{\sigma}_{2ac}$ tends to saturate. This could explain the larger cross-sections measured by Norton [18] with respect to those obtained by Levitt-Honig [19]. It is important to stress that the uncertainty in the definition of the capture cross-section (see eq. (16)) reflects the uncertainty in the experimental measurements of τ_r. As we have shown above, there is no rigorous definition of this quantity and, as a matter of fact, different experimental methods give different values for τ_r. Let us consider, for example, the case when τ_r is derived by measuring the relaxation of photoconductivity after far-infrared excitation of carriers from impurities to the conducting band. In this experiment the population of excited impurity levels plays a decisive role. As a consequence, if the measurements are performed at the long time tail of the current relaxation, it is possible to measure recombination times close to τ_{r2}. On the other hand, if the measurements are performed just after the pulse light is switched off, recombination times close to τ_{r1} are measured. In this last case an initial fast decrease of the current relaxation is associated with capture of carriers by the excited impurity levels. However, after an elapsed time of the order of several τ_{r1}, carrier generation from these excited levels becomes important. This leads to a subsequent slower decrease of the current relaxation which implies a longer recombination time. Therefore, any characteristic time between τ_{r1} and τ_{r2} may be measured depending on the light pulse duration, on the interval of time used for measuring the current relaxation and on the delay time after the light pulse is switched off. In the old experiments available from the literature researchers did not pay attention to these

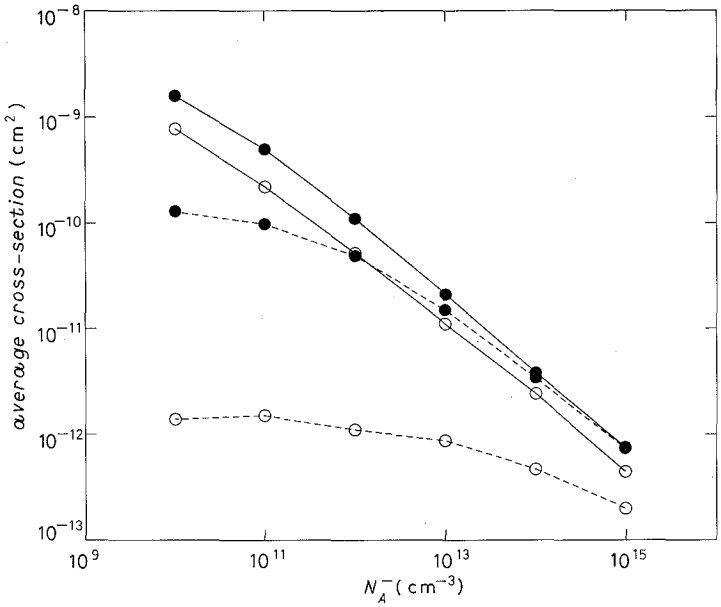

Fig. 12. – Average capture cross-section in p-type Si as a function of the ionized acceptor concentration as obtained from the Monte Carlo simulation. Full and open circles refer to the temperatures $T = 2$ and 10 K, respectively. Continuous and dashed curves refer to $\bar{\sigma}_{1ac}$ and $\bar{\sigma}_{2ac}$, respectively (see the text).

peculiarities, thus it is actually impossible to clarify which time was originally determined.

6. – Conclusions.

In this paper we have presented a molecular dynamics calculation as a novel numerical method to study the recombination cross-section of free carriers at ionized shallow centres assisted by acoustic phonons. The essence of the method enables us to avoid any approximate solution of the kinetic equation and clarify the fundamental importance of excited levels in the determination of the capture cross-section. The theory is specialized for the case of p-type Si at different temperatures and ionized acceptor concentrations. The satisfactory agreement obtained with available experiments and the clarity of the physics underlying the calculations gives us confidence in predicting that this technique will be further developed to account for refinements in the theory.

* * *

This work has been performed on the basis of a Scientific Cooperation Agreement between the Academy of Sciences of the USSR and the National Research Council (CNR) of Italy. Partial support is provided by Ministero dell'Università e della Ricerca Scientifica e Tecnologica (MURST) and the Centro di Calcolo of the Modena University. Authors acknowledge Drs. Tilmann Kuhn of the Modena University and Carolyne Van Vliet of the Montreal University for valuable discussions on the subject.

REFERENCES

[1] M. LAX: *Phys. Rev.*, **119**, 1502 (1960).
[2] V. N. ABAKUMOV and I. N. YASSIEVICH: *Sov. Phys. JETP*, **44**, 345 (1976).
[3] V. N. ABAKUMOV, V. I. PEREL and I. N. YASSIEVICH: *Sov. Phys. Semicond.*, **12**, 1 (1978).
[4] I. N. YASSIEVICH: in *Semiconductor Physics*, edited by V. M. TUCHKEVICH and V. Y. FRENKEL (Plenum, New York, N.Y., 1986), p. 519.
[5] R. A. BROWN and S. RODRIGUEZ: *Phys. Rev.*, **153**, 890 (1966).
[6] F. BELEZNAY and G. PATAKI: *Phys. Status Solidi B*, **13**, 499 (1966).
[7] R. A. BROWN and S. RODRIGUEZ: *Phys. Rev.*, **153**, 890 (1967).
[8] W. PICKIN: *Phys. Rev.*, **20**, 2451 (1979).
[9] W. PICKIN: *Phys. Status Solidi B*, **96**, 617 (1979).
[10] E. M. GERSHENZON, G. N. GOLTSMAN, V. V. MULTANOVSKII and N. G. PTISYNA: *Sov. Phys. JETP*, **50**, 728 (1979).
[11] G. L. J. A. RIKKEN, P. WYDER, J. M. CHAMBERLAIN and L. L. TAYLOR: *Europhys. Lett.*, **5**, 61 (1988).
[12] B. RÖHRICHT, R. P. HUEBENER, J. PARISI and M. WEISE: *Phys. Rev. Lett.*, **61**, 2600 (1988).
[13] F. A. KHAN and D. P. BHATTACHARYA: *Solid State Commun.*, **51**, 719 (1984).
[14] L. REGGIANI, P. LUGLI and V. MITIN: *Appl. Phys. Lett.*, **51**, 925 (1987).
[15] L. REGGIANI, R. BRUNETTI and E. NORMANTAS: *J. Appl. Phys.*, **59**, 1212 (1986).
[16] C. JACOBONI and L. REGGIANI: *Rev. Mod. Phys.*, **55**, 645 (1983).
[17] L. REGGIANI and V. MITIN: *Rivista Nuovo Cimento*, **12**, No. 11 (1989).
[18] P. NORTON, T. BRAGGINS and H. LEVINSTEIN: *Phys. Rev. Lett.*, **30**, 488 (1973).
[19] R. S. LEVITT and A. HONIG: *J. Phys. Chem. Solids*, **22**, 269 (1961).